Mixing of biomass particles in fluidised beds combustors and gasifiers

Candidate no. 15065

1 Description of the gasification process

Biomass is an abundant energy source and its exploitation to produce thermal or electrical energy is currently highly considered and investigated worldwide. The most promising technology for that is the gasification in fluidized or fixed bed reactors, with the aid of gasifying media like hot air, steam etc. Gasification of biomass is a thermochemical decomposition procedure that produces syngas CH_4 and other chemical feedstocks [1]. Syngas can then be used to produce other feedstocks, like methanol, and has numerous applications [2]. The main advantage of gasification against combustion is that the produced gas can be efficiently cleaned-up and conditioned before its usage, and thus is much less harmful to the environment or to downstream equipment [3].

Fluidized Bed Gasifier (FBG) seems to be advantageous over gasification technologies (e.g. fixed bed), due to its flexibility to handle broad variety of biomass type, particle size and quality, with stable operation and high conversion efficiency [4], reported up to 95-98% [5], [6], provided that the mixing of biomass in the bed is very good, and thus adequate heat and mass transfer between the inert and the biomass particles is secured. Moreover, it achieves high availability, above 90% [3], as it operates with continuous introduction of new biomass fuel [5], it allows load variation and fast heat-up, and it can be constructed in large sizes and power rate [7]. The operation temperature is relatively low (usually 800 to 900 °C), a compromise to prevent melting of inert bed material and ash components, and to achieve good biomass conversion efficiency. [5], [8].

There are two main types of FBs (Fig. 1a): Bubbling and Circulating [2], [3]. Bubbling beds have relatively low gas velocities, so as only few solids are conveyed with the outflow gas, whereas Circulating beds use higher velocities causing pneumatic transport of solids that are then collected in a cyclone and recycled to gasifier [3]. Several other strategies and configurations are currently being investigated, like entrained bed, multistage gasification, pyrolysis and gasification at different locations, supercritical water gasification and plasma gasification [2], [9]. The main parts of a FB gasifier are shown in Fig. 1a: The gasification chamber is partially filled with small inert particles (silica, sand, lime, etc.), and hot gas is injected at the bottom, so as above certain flow rate the bed material starts to behave as a fluid. Biomass enters through side or bottom feeders, and the residual ash is removed mainly from the bottom, while some lither particles are collected in a cyclone.

The operation principle is as follows: At low fluidisation velocities the bed behaves as static porous media (fixed bed), and the pressure drop increases almost linearly with the velocity (Fig. 1b). There is a certain velocity value above which the entire bed material (inert and biomass particles) start to behave as a liquid, and this is called minimum fluidisation velocity U_{mf} [2], [10]. Above that value bubbles start to appear in the bed, transferring the excess fluidising gas quantity. When the bed is fully fluidised and it is vigorously bubbling, the pressure drop remains constant (Fig. 1b). The intersection of these two pressure lines can be considered to define the minimum fluidisation velocity (U_{mf}) of the bed [10], [11].

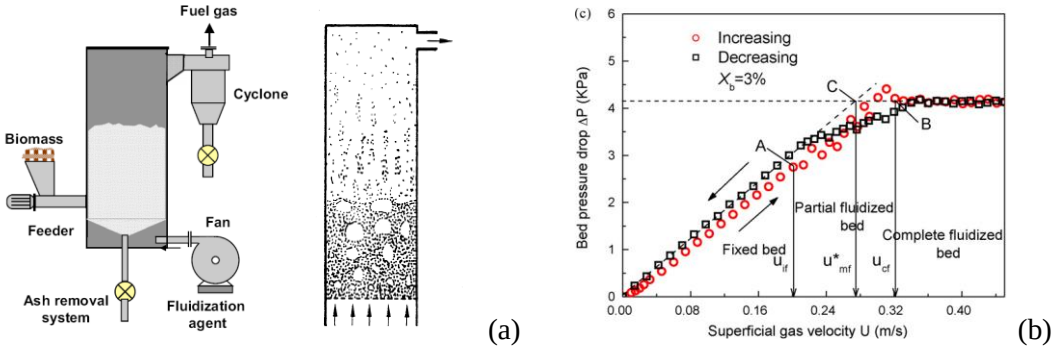

Figure 1. (a) Bubbling fluidized bed [A6]; (b) Pressure drop in a FB [A12].

2 Requirements for successful combustion/gasification

The performance of a FBG as well as the quality and properties of the gas product are dependent on several key parameters. The parameters that are mostly met in the literature are the feedstock material type, particle size, the moisture content, the gasifying agent type, the superficial velocity, the feedstock dimensions, the temperature and pressure inside the bed, design and dimensions of the gasifier, and the presence of catalyst and sorbent material [2]. Higher temperatures in the FB facilitate the conversion of char to gas and reduce the formation of tar and the concentration of higher hydrocarbons (char) in the produced gas [12], [13], [5].

Moisture content of the biomass fuel is also important because it affects strongly the temperature in the bed, as evaporation absorbs energy and reduces the FB temperature. Furthermore, the quality of the produced gas becomes lower as its water vapor content increases [13]. The moisture content of the feedstock must be low enough, usually below 30% [3] in order for the process to be self-sustainable. Higher moisture content biomass requires external heat source or special drying equipment that would increase the complexity and cost of the FB gasifier. As a result, green biomass, which is the most abundant and cheap, cannot be used [3].

Another important aspect of a gasifier is the content in ash and tar. The ash and tar content of biomass melts at relatively low temperature and can cause deposition and agglomeration in the bed, as also fouling and corrosion/slagging problems in the downstream equipment of the gasifier [8], [4]. Special bed materials or additives to control this mechanism are yet to be discovered.

Biomass particle size also plays an important role because the heating rate is higher in smaller fuel particles due to their greater surface (for same mass). Therefore, the gasification process generally improves as the fuel particle decreases. Also, the controlling parameter of gasification is different: In small particles the rate is mainly determined by reaction kinetics, while in large particles by the diffusion rate of the gas produced inside the particle [13]. Biomass density is usually smaller than the inert bed material and hence the particles are subjected to upward beyond force that tends to transfer the to the surface (axial segregation).

The fludisation agent can be air or combination of steam with air or with oxygen. The syngas produced with air has lower heating value due to the nitrogen content, whereas steam and oxygen produce better heating value syngas [5]. Use of suitable air-steam mixture can produce gas with higher hydrogen content [14]. CO_2 has been also used as agent and found to increase H_2 and CO concentration and high heating value gas [15] [16]. Therefore, the calorific value of the product gas depends on the fluidization agent. The latter has also an important role in the conversion of char and heavy hydrocarbons (HC) to lighter gases such as carbon monoxide (CO) and H_2 [2]. The superficial velocity of the fluidizing gas is the controlling factor for mixing and segregation behaviour of biomass particles in the bed. Typically, its value is of the order of 0.5 m/s. Lower values result in slower gasification and hence higher char and tars [5].

The use of additives constitutes an important factor of gasification. Chlorides and sulphurous gas components can be removed by sorbents such as CaO and ZnO. Tar is subsequently cracked in the presence of catalysts.

3 Types and properties of materials

3.1 biomass particles

The effectiveness, efficiency and product quality of a FBG are critically dependent on the chemical composition and moisture content of biomass material, which affect its reactivity and kinetics of thermal decomposition, as well as the composition and calorific value of the produced gas, the char and tar yields, and the environmental impact. Biomass resources can be classified in various ways, depending on their purpose. In respect of resource magnitude, availability, energy content and cost, there are two main classes: Rural and Urban resources [3]. There are various biomass classifications and their relative usefulness which are based on its biological diversity, source and origin [2]:

a) Wood (most commonly used biomass. Low and controllable moisture content. Minimum Sulphur and heavy metals. Forest biomass is ideal for gasification due to high cellulose and hemicellulose percentages.
b) Agricultural and herbaceous biomass (grasses, straws, others (grains, pulp, etc.). Year-round availability and cost-effectiveness, but high moisture content.

c) Marine biomass (algae). Intense research to obtain biofuels/biodiesel (3rd, 4th generation). Genetically modifiable to reduce further C-trace.
d) Human and animal waste. Potential to produce energy in BF and other useful chemicals.
e) Contaminated and industrial waste biomass. Possible syngas production by gasification.
f) Mixtures of the above to obtain desirable properties.

Classification based on the biomass particle density and/or size can be also used, as far as these properties affect the mixing and segregation mechanisms in the FB.

3.2 Inert materials

The most common inert bed material is silica, that has high strength and heat capacity. However, some other inert solids such as, sand, olivine, glass beads, dolomite etc. that has also some catalytic behaviour that reduces tar formation problems are currently examined [5]. The ability to fluidise and the fluidising behaviour of particles (minimum fluidization velocity, bubbles size and velocity) depends mainly on their size and density. A generally used classification of Geldart (1973) [17] defines four different powder types:

1. Group A (aeratable): small size and low density (mean $d_p < 100$ μm, $\rho <\sim 1.4$ g/cm^3). Fluidise easily at low gas velocities with formation of bubbles at velocities always above U_{mf}. Fluid cracking catalysts are in this class.
2. Group B (sand-like): size 150 μm to 500 μm and density from 1.4 to 4 g/cm^3. For these particles, once the minimum fluidization velocity is exceeded, the excess gas appears in the form of bubbles.
3. Group C (cohesive): very fine powders $d_p < 30$ μm, extremely difficult to fluidize (large interparticle forces)
4. Group D (spoutable): either very large or very dense. They are difficult to fluidize in deep beds. As velocity increases, a jet can be formed in the bed and material may then be blown out with the jet (channelling) [18].

4 Physical mechanism of mixing and segregation

Fluidised bed is a well stirred and controllable environment for heterogeneous and gas-phase reactions, but these features are not retained when it is used to process biomass [19]. The size of biomass particles is usually much larger than that of the inert solids, and their density much lower. These differences lead to a very complex and difficult to predict motion and distribution of biomass fuel in the bed, which is affected by many design and operating parameters.

In any case, good mixing and minimization of segregation is required in order to achieve efficient thermal control and maximize the conversion efficiency of a FBG, as also to optimize its performance in terms of O&M costs and environmental impact.

There are various types of multiphase flow field that can be developed in FB gasifiers, and various mixing processes due to convection and diffusion (bubbling, circulation, axial and lateral mixing of solids and gas, upward/downward motion of particles, etc.).

4.1 Mixing mechanisms

The mixing rate of biomass fuel with the inert bed particles is of crucial importance because it controls the heat transfer to the biomass particles, and also the mass transfer of the gases throughout the bulk bed material. Vertical and lateral mixing can produce a more uniform temperature field, with the aid also of the thermal inertia of the bed solids [20]. The rising gas bubbles through the bed is the principal factor that activates and governs the mixing of solid particles, via three main mechanisms [21]:

A. A bubble drags some solids in its wake volume, due to the lower pressure developed there. The volume of this wake, and hence the transport capability can be up to 1/3 in group A particles, and decreases towards Group D (Geldart, 1986) [22].
B. A rising bubble create a cycling motion of the bed material that is sinks around the bubble to fill the created gap. These vertical circulation pathways around the bubbles are called ‘mixing cells’ [20], [20] (Fig. 2). A mixing cell consists of the wake phase, where the solids are carried to the top in the bubble wake, and the solid phase, where the solids leave the wake and flow down [21]. Exchange of material takes place between adjacent cells (drift sinking) [23].

C. When the bubbles reach at the bed surface they erupt creating splashing (splash region) and dispersing around the carried solids in its wake [1], [24].

The first mechanism is responsible for the upward motion and mixing of the particles, whereas the other two control the lateral mixing. The bed dimensions affect the strength of the above mechanisms. The lateral dispersion coefficient increases for higher gas fluidization velocity and bed height [25], [20], while the splashing predominates in shallow beds [26].

In typical gasifiers, vertical mixing is about one order of magnitude stronger than lateral mixing [20], while lateral dispersion and mixing is mainly controlled by the exchange rate of particles among adjacent mixing cells [1]. The experimentally obtained values in laboratory models for the lateral dispersion coefficient are much different, and vary in the range of 10^{-4} to 10^{-1} m^2/s. However, in large scale FBG, the dispersion coefficient can be much larger than in scaled models (0.1 m^2/s), [20].

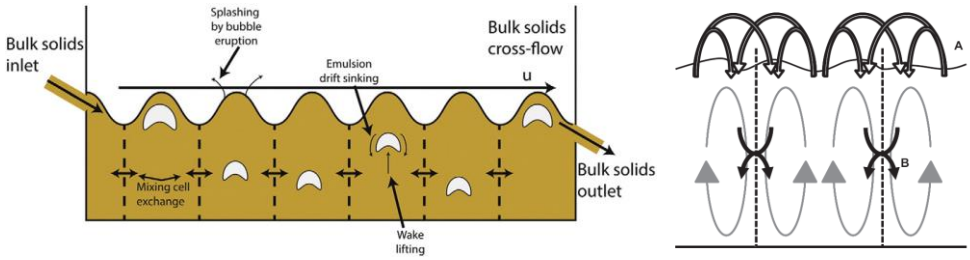

Figure 2. Lateral solids mixing due to the mixing cells and bubbles eruption.

Mixing of volatile matter in the bed via various mechanisms (macro- meso- and micro-mixing, [1]) is important in FB combustors, where a more uniform distribution of released gas allows for relatively low combustion temperatures (flameless combustion), and hence reduces pollutant emissions [1]. This feature is not required in FB gasifiers where no combustion takes place. However, the endogenous vapour bubble created around a biomass element may accelerate its upward motion and enhance the segregation at the bed surface [27], therefore its fast mixing rate in the bed environment is desirable.

4.2 Segregation mechanisms

Segregation of biomass particles in a particular area of the bed is a competitive to mixing mechanism that can deteriorate the conversion effectiveness and efficiency of the gasifier, because it obstructs the direct contact of biomass with the hot bed particles, and hence the heat transfer rate to them is reduced. Strong segregation in FBG can occur if there are particles in the bed with different physical properties, mainly density but also size [21], [26]. Lighter or finer particles migrate to the bed surface and constitute the "flotsam" phase, while the larger and heavier particles are the "jetsam" phase and tend to accumulate at the bottom. Jetsam settling rate is faster than flotsam rate for particles of equal relative density. This is because jetsam phase can fall down through bubbles and remain temporarily in the disturbed flow below them [21].

In FBG, vertical segregation of biomass elements is controlled by various different mechanisms [11], depending on the operating conditions:

Percolation effect: It is a local mechanism by which the finer bed particles flows under the larger biomass elements, due to some small vibrations caused during the expansion of the bed, just before it becomes fluidized.

Buoyancy: The fluidised bed behaves like a liquid and hence a submerged lighter biomass particle is subjected to buoyancy force that is larger than its gravity force, hence the net upward force. This vertical segregation mechanism initiates at small gas velocities, even without the presence of bubbles.

Bubbles: The most controlling parameter of the vertical segregation (like of the mixing rate) is the rising bubbles. For relatively low gas velocities above minimum fluidization speed, the bubbles drag the biomass and bed particles in their wake and transport them to the bed surface [21]. Then, the lighter biomass particles remain and segregate there. However, for higher gas velocities the number of rising bubbles increases and the top layer of the bed becomes strongly splashing, enhancing mixing of biomass there [11]. Moreover, the coalescence of bubbles creates larger

slugs and voids in this layer, in which both inert and biomass particles can fall and move fast downwards. This mechanism can counteract segregation and as a result, the overall mixing index of the bed increases [11].

Endogenous bubbles: These are formed due to volatiles release and surround a biomass particle, thus increasing its buoyancy and its rising speed. A biomass particle can be lifted to the bed surface by a single such bubble or as a result of the action of multiple bubbles (single or multiple bubble segregation, [1], [28]). This mechanism is more effective for lighter particles or for particle with higher devolatilization rate [1], [27]. Moreover, as long as this endogenous bubble surrounds the particle, the mass transfer to the emulsion phase is obstructed.

Fragmentation and attrition of biomass particles: This is caused due to the mechanical stresses (collisions, attrition) of particles as they move in the dense bed of inert solids, especially during volatiles release and gasification of char, which are shrinking the particles and weakening its bonds [7], [29]. Moreover, the mechanism results in reduction of mean biomass particles size and creation of fine particles that are transported faster to the surface by the fluidizing gas.

The time scale of vertical (axial) segregation (t_{AS}) is of the order of 1s (typical bubble rise velocities and bed height of the order of 1 m/s and 1 m, respectively [1], which is usually smaller than the devolatilisation time scale of biomass particles (t_D), regardless of their size [1]. Consequently, if this mechanism prevails, the efficiency of the bed is reduced.

Reduction of axial segregation rate can be achieved by promoting internal circulation and mixing of the bed solids, by using heavier and larger biomass particles, by increasing particle moisture content (up to a limit), and by improving the design of fuel feeding conditions [30].

Lateral segregation can also occur, caused mainly close to the biomass feeding port side of the bed, and when the lateral spreading time t_{LS} (or lateral dispersion rate) is much smaller than the devolatilization time. In that case, the volatile gas is concentrated close to the feeding point and transferred by the fluidising gas to the bed surface, with possible formation of 'plumes' [7]. The spreading time of biomass is given according to an approximate relation [30]: $t_{LS} \approx L^2/2D$, where L is the bed width and D the diffusion coefficient. For large scale FBG this relation gives a spreading time of the order of minutes, quite higher than t_D for particles up to 10 mm, therefore the enhancement of lateral dispersion is important in order to increase the efficiency of large scale units.

If axial segregation is significant, the splashing at the bed top layer can enhance the lateral mixing [1]. However, it was found that in large scale FB lateral mixing is more pronounced in the dense bed between the mixing cells than at the surface, and therefore, higher fluidization velocities improve further the mixing effect of these circulating vortices [23] and enhances the migration of the biomass particles from the feeding point towards the centre of the bed [31].

Better lateral mixing can be also achieved by increasing the number of biomass feeding ports. This should be preferable in case of high volatile fuels or of large bed widths [32]. However, design constraints and cost generally limit the number of feeding ports even in large-scale FB units [27]. Large scale circulation of bed particles and/or induced lateral flow of fluidised solids could also reduce lateral segregation.

5 Properties of FB material and bubbles

Numerous theoretical and empirical correlations have been proposed by many researchers, in order to estimate the properties and behaviour of the bed material and the gas bubbles as function of its composition and operating conditions. For the present simulation the following are adopted:

The apparent density the bed is obtained considering it as a mixture of gas and particles [33]:

$$\rho_{app} = \rho_f \left(1 - \varepsilon_p\right) + \rho_{app}\, \varepsilon_p \tag{1}$$

where ρ_f and ρ_p are the density of the gas and the bed particles, and e_p the particle volumetric concentration in the bed. The apparent viscosity bed material can be obtained from the relation [33]:

$$\mu_{app} = \mu_f \left(1 - \varepsilon_p\right)^{-2.8} \tag{2}$$

where μ_f is the viscosity of the fluidizing gas. According to the two-phase theory of fluidization proposed in [34], if the gas velocity exceeds the minimum fluidization velocity, all the additional gas quantity is injected in the form of bubbles. Therefore, the bubbles flow rate will be:

$$Q_b = n\, V_b = A \left(U - U_{mf}\right) \tag{3}$$

where n is the number of bubbles per second (assumed of equal size), V_b the bubble volume, and A the horizontal cross section area of the bed. The size of the bubbles is also depended on the superficial gas velocity, as also on the orifice type and structure and the distance from the injection level.

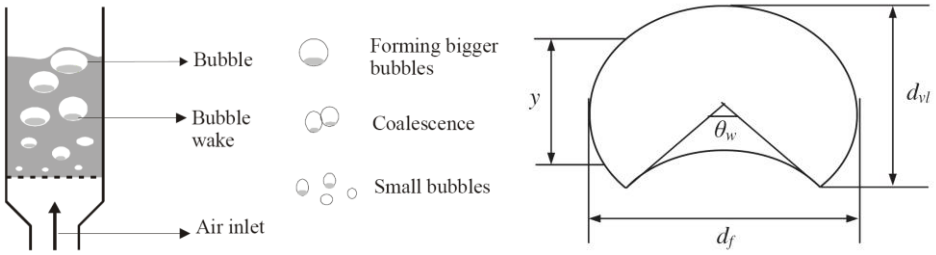

Figure 3. Evolution and characteristic shape of bubbles in a FBG [35].

The size of the bubbles is depended on the superficial gas velocity, as also on the orifice type and structure, and the distance from the injection level. Several empirical correlations of various researchers for the bubble size and velocity are reviewed in [35]. A commonly used expression for *initial* diameter (in cm) of a single bubble formed in porous distributor is [35]:

$$d_0 = 0.00376\left(U - U_{mf}\right)^2 \tag{4}$$

As the bubbles move upwards in the fluidized bed, they are coalescing (Figure), and fewer and larger bubbles are created. The correlation of [15] that models this mechanism is adopted:

$$d_f = \left(U - U_{mf}\right)^{1/2}(h + h_s)^{3/2}/g^{1/4} \tag{5}$$

where d_f is the bubble width (Figure), h is the vertical distance from the orifice, h_S is close to zero for porous plate distributor [15], g is the gravity acceleration, and all quantities are in cm.

The volume averaged diameter of the bubble is $d_b \approx 0.9\ d_f$ [35]. A correlation for the rising velocity of a single bubble is taken from [35], among several others proposed in the literature:

$$U_b = 0.71\ (g\ d_b)^{1/2} \tag{6}$$

Hence, the rising velocity of bubbles increases as they move upwards and become fewer and larger. Finally, the expansion of the bed due to the presence of the bubbles can be obtained by combining the above relations, as:

$$h/h_{mf} = 1 + \left(U - U_{mf}\right)/U_b \tag{7}$$

where h_{mf} is the bed minimum fluidization height (without bubbles).

6 Modelling of FB operation and mixing procedure

Modelling of the very complex gasification process and the several physical and thermochemical mechanisms involved is still a big challenge in international research. The various models can be classified in thermodynamic equilibrium, kinetic, CFD with Eulerian and/or Lagrangian approach, and ANN [2], [13], while several experimental works have been performed mainly in scaled down laboratory models [10].

6.1 The Smoothed Particle Hydrodynamics model

The Smoothed Particle Hydrodynamics (SPH) is a meshfree method which represents a set of particles with individual properties and attempts to model their motion according to the governing equations of a problem. It was firstly developed by Lucy (1977) and was subsequently used by Gingold and Monaghan (1977) [36] for the solution of astrophysical problems, like the motion of stars and other celestial bodies in 3-dimensional space. The method was extensively studied and extended (Monaghan 2005) for dynamic response with material strength as well as the hydrodynamic modelling of fluid flow problems. The meshfree nature of the method allows for a faster and less computationally expensive simulations of particle motion compared to other methods like FEM or CFD, and provides high adaptivity for problems that involve extreme deformations [36]. Another attractive feature of the method is its capability to simulate free surface flows as well as flows that include interface interactions of two or more different fluids [36]. For these reasons it was selected for the simulation of the fluidized bed for the current study.

SPH attempts to provide a solution for the partial differential equations (PDEs) that govern a hydrodynamic problem which include variables such as the density, velocity and the displacement of a particle [36]. The degree of interaction between a particle and the rest of the particles in the computational space would be extremely time-inefficient, thus the accounted interaction involves only particles that lie within a predefined neighbouring area.

Let *f(x)* be a function that defines a property of a fluid. For a given particle *i* the value of *f* is given by:

$$f(x_i) = \int f(x_j) W_{ij} d\vec{r}_{ij} \tag{8}$$

where *j* is a neighbouring particle, $f(x_j)$ the value of *f* for particle *j*, *W* the smoothing kernel function and $\vec{r}_{ij}$ the distance between the two particles. The above equation and its derivative can be expressed in its SPH form as:

$$f(x_i) = \sum_{j=1}^{N} \frac{m_j}{\rho_j} f(x_j) W_{ij} \tag{9}$$

$$\nabla \cdot f(x_i) = -\sum_{j=1}^{N} \frac{m_j}{\rho_j} f(x_j) \nabla \cdot W_{ij} \tag{10}$$

where

$$W_{ij} = W(x_i - x_j, h) \tag{11}$$

with *h* being the smoothing length of a cell that belongs to an auxiliary grid which defines the influence area of the smoothing function *W* and m_j, ρ_j the mass and density of particle *j*, respectively. The discretised values of *W* can be found from:

$$W(q) = \frac{a_d}{h^d} \begin{cases} (2.5-q)^4 - 5(1.5-q)^4 + 10(0.5-q)^4, & 0 \le q \le 0.5 \\ (2.5-q)^4 - 5(1.5-q)^4, & 0.5 \le q \le 1.5 \\ (2.5-q)^4, & 1.5 \le q \le 2.5 \\ 0, & q \le 2.5 \end{cases} \tag{12}$$

where q is the ratio of $|r|/h$. The kernel pattern and the auxiliary grid are given in Fig.4a and 4b, respectively.

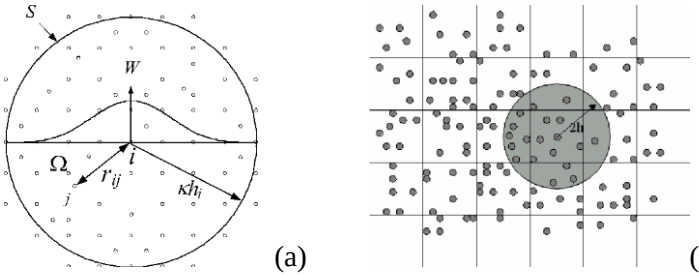

(a) (b)

Figure 4. The kernel interaction smoothed function (a) and the auxiliary grid for particle tracking (b).

Finally, the SPH flow equations that are solved for each *dt* using the numerical method of Prediction-Correction are the continuity and momentum, given by:

$$\frac{d\rho_i}{dt} = \sum_j m_j u_{ij} \nabla \cdot W_{ij} \tag{13}$$

$$\frac{du_i}{dt} = -\sum_j m_j \left[\left(\frac{p_i}{{\rho_i}^2} + \frac{p_j}{{\rho_j}^2} \right) \nabla \cdot W_{ij} - \Pi_{ij} \right] + g \tag{14}$$

where Π_{ij} is a viscosity term and g is the gravitational acceleration.

6.2 Case study

The experimental set-up of [11] is selected for the numerical simulations with the SPH computer code. The design and operation characteristics of this set-up are as follows:

Bed dimensions	Rectangular base, 0.4x0.4 m^2, Height 0.3 m (inert only)
Inert particles	Quartz sand, spherical, 0.5 mm mean diameter
Particle volume concentration	$\varepsilon_p = 0.456$
Static bed density	1393 kg/m^3
Biomass particles	Cotton stalk, cylindrical, 5mm x 50 mm, density: 385 kg/m^3
Biomass mass concentration	1% - 3%

Using these data and the above correlations, the bed viscosity becomes: $\mu_{app} = 1\text{x}10^{-4}$ Ns/m^2, while the bubble properties can be obtained based on the difference between superficial and minimum fluidization velocity ($U - U_{mf}$). For example, for a difference of 0.6 cm/s the bubble volumetric diameter at a half bed height of $h \approx 20$ cm will be about 3.6 cm (eq. 5), and the bubble rising velocity from eq. (6) will be: $U_b \approx 42$ m/s. Then, the number of bubbles per second can be obtained from eq. (3), in a 2-dimensional approach, becomes: $n \approx 20$ bubbles/sec, and the expanded bed height (eq. 7) becomes: $h \approx 40$ cm (including 3% biomass material concentration).

For the present SPH simulations, the size and velocity of the bubbles are kept constant to the average values along the entire bubble path. Also, the different density of biomass particles is taken into account by changing analogously the acceleration of upon them.

6.3 Numerical results

Some indicative snapshots from the simulation with the developed SPH algorithms are shown in Fig. 5. Initially, the cylindrical biomass particles are uniformly distributed in the bed, as in [11]. Then the bubbles start to rise and create a complex motion of the inert and biomass particles in the bed (Fig. 5b). After several seconds, in this particular case of small bubbles flow rate (20 bps), all biomass particles are transported to the bed surface, due to their much lower density (Fig. 5c).

The mixing is slightly improved when the superficial speed increases and more bubbles are injected (50 bps), as shown in Fig. 6a. However, a significant improvement even with only 20 bps, when the bubbles are injected in fixed columns, instead of randomly (Fig. 6b compared to Fig. 5c), due to a stable circulation and downward flow that is established between the columns.

Other remarkable features of the present simulation is that the results reproduce the expansion of the bed material depending on the superficial velocity (bubbles flow rate), as also that the increase of the bubbles volume as they approach the surface, due to the reduction of hydrostatic pressure, though a bubble is always represented with the same number of particles (here 10, Fig. 6c).

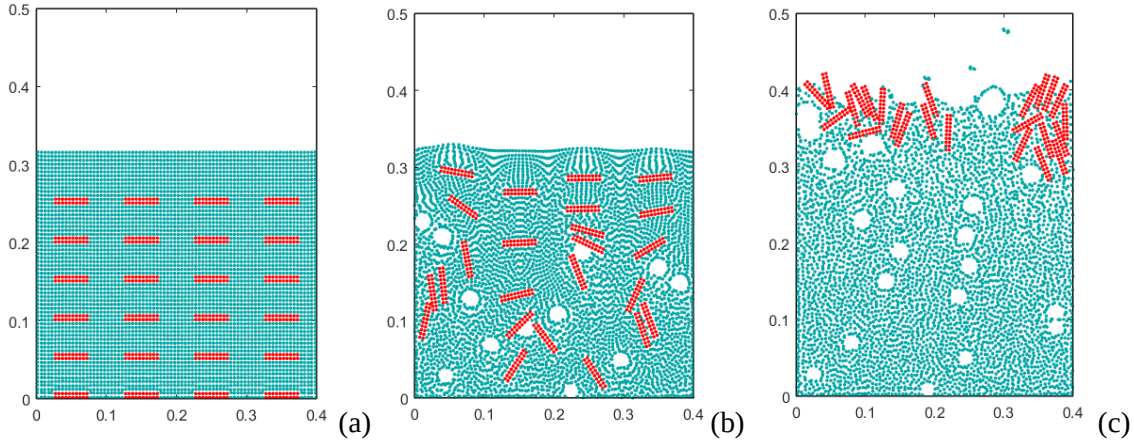

Figure 5. Indicative pictures of the mixing progression in the bed for 20 bubbles/s.

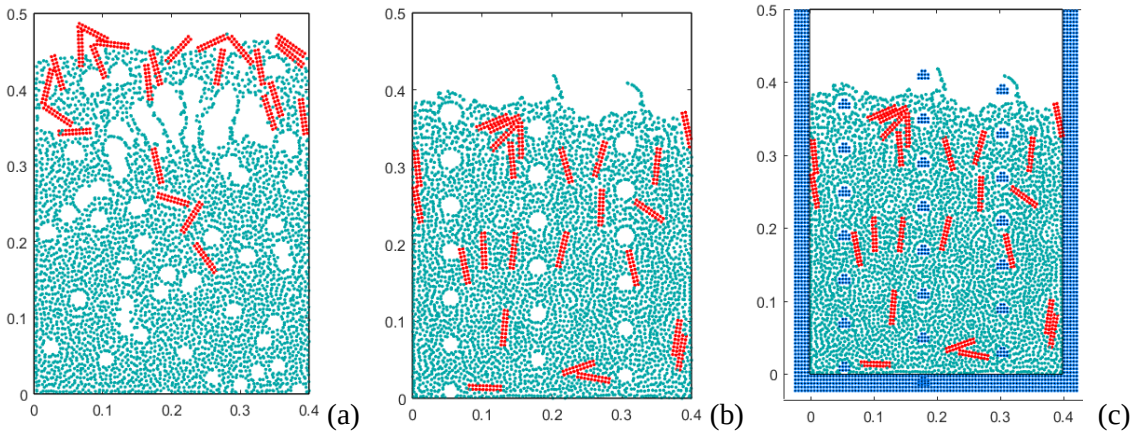

Figure 6. Final mixing: (a) 50 bubbles per sec; (b) 20 bps; (c) boundaries and bubbles shape.

The algorithm is then applied to a specific case of [11], with 3% biomass concentration, to obtain the mixing index, *M*, for various values of the excess gas velocity ($U–U_{mf}$). For each simulated value the bubbles size, low rate and rising velocity are recomputed as in the example above (the minimum bubble shape has 2x2 particles and the maximum has 5x4). The convergence of this index is not quite smooth, but it tends to stabilize after about 30 seconds (Fig. 7a). The results in Fig. 7b agree with the measurements for small excess gas velocity (close to zero), but the predicted mixing increases faster, to about 0.8 for 12 cm/s, which is achieved for much higher gas velocities in [11]. It seems that 2D simulation may overestimate the mixing effect of rising bubbles, since the lengthy biomass particles cannot avoid them.

Then, the simulations are repeated for the same bubble rate but in columns, showing a much better mixing with small excess velocity, which however reduces for higher values, possibly because the increasing viscous friction of the rising bubbles affects negatively the downward circulation of the large biomass particles. Finally, a case with small biomass particles (single points) is simulated and the resulting curve in Fig. 7b shows that an almost perfect mixing can be achieved at relatively small excess gas velocity.

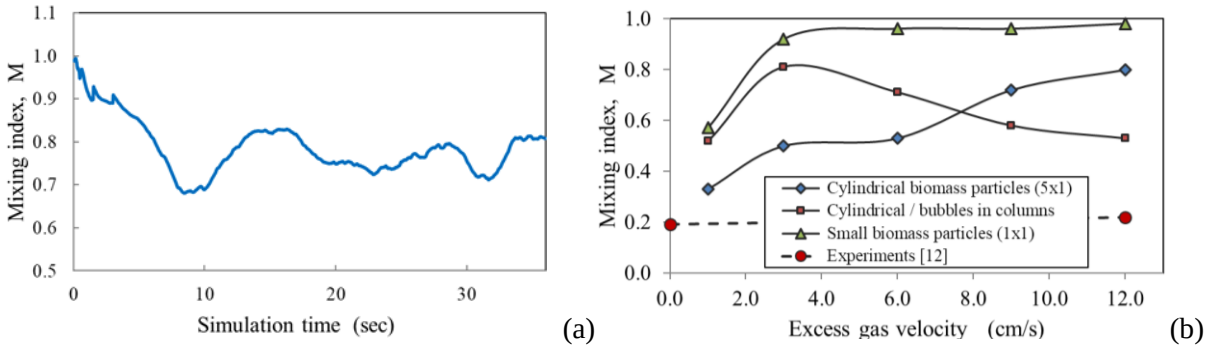

Figure 7. (a) Mixing index time variation; (b) Final mixing results for various examined cases.

7 Conclusions and Proposals

From the literature studies and results it can be deduced that enhancement of mixing and reduction of axial segregation rate is essential for an optimum and efficient design of a FBG. This can be achieved by promoting internal circulation and mixing of the bed solids, by using heavier and larger biomass particles, by increasing particle moisture content (up to a limit), and by improving the design of fuel feeding conditions.

The present simulation results showed that the use of properly distributed columns of rising bubbles throughout the bed, instead of a random generation, can improve significantly the mixing of biomass and reduce axial segregation, using smaller superficial gas velocity and energy. The observed behaviour in the present 2D simulations is expected to be valid in 3-Dimensions too, where however the computational effort to optimize the circulation would be much greater. A second outcome is that small size of biomass particles can be mixed much more efficiently than large and non-symmetric particles. It is recommended to perform corresponding experiments in order to validate these findings.

The SPH model is able to simulate with relatively simple computer algorithm the very complex unsteady multiphase flow field in a FBG, including gas bubbles and biomass particles of various size and shape, and producing quite realistic results. Consequently, it is strongly proposed for further studies and more elaborated modelling, in order to improve the accuracy and applicability of its results and thus create a powerful tool for the future development of FBG technology.

8 References

[1] Piero Salatino and Roberto Solimene. Mixing and segregation in fluidized bed thermochemical conversion of biomass. *Powder Technology*, 316:29–40, 2017.

[2] Vineet Singh Sikarwar, Ming Zhao, Peter Clough, Joseph Yao, Xia Zhong, Mohammad Zaki Memon, Nilay Shah, Edward J Anthony, and Paul S Fennell. An overview of advances in biomass gasification. *Energy & Environmental Science*, 9(10):2939–2977, 2016.

[3] U EPA. Biomass combined heat and power catalog of technologies. *Washington DC, US EPA Google Scholar*, 2007.

[4] AA Khan, W De Jong, PJ Jansens, and H Spliethoff. Biomass combustion in fluidized bed boilers: potential problems and remedies. *Fuel processing technology*, 90(1):21–50, 2009.

[5] SK Sansaniwal, K Pal, MA Rosen, and SK Tyagi. Recent advances in the development of biomass gasification technology: A comprehensive review. *Renewable and Sustainable Energy Reviews*, 72:363–384, 2017.

[6] Marcin Siedlecki, Wiebren De Jong, and Adrian HM Verkooijen. Fluidized bed gasification as a mature and reliable technology for the production of bio-syngas and applied in the production of liquid transportation fuelsa review. *Energies*, 4(3):389–434, 2011.

[7] Alberto Gómez-Barea and Bo Leckner. Modeling of biomass gasification in fluidized bed. *Progress in Energy and Combustion Science*, 36(4):444–509, 2010.

[8] Ragnar Warnecke. Gasification of biomass: comparison of fixed bed and fluidized bed gasifier. *Biomass and bioenergy*, 18(6):489–497, 2000.

[9] Antonio Molino, Simeone Chianese, and Dino Musmarra. Biomass gasification technology: The state of the art overview. *Journal of Energy Chemistry*, 25(1):10–25, 2016.

[10] TJP Oliveira, CR Cardoso, and CH Ataíde. Bubbling fluidization of biomass and sand binary mixtures: Minimum fluidization velocity and particle segregation. *Chemical Engineering and Processing: Process Intensification*, 72: 113–121, 2013.

[11] Yong Zhang, Baosheng Jin, and Wenqi Zhong. Experimental investigation on mixing and segregation behavior of biomass particle in fluidized bed. *Chemical Engineering and Processing: Process Intensification*, 48(3):745–754, 2009.

[12] Afsin Gungor. Modeling the effects of the operational parameters on h2 composition in a biomass fluidized bed gasifier. *international journal of hydrogen energy*, 36(11):6592–6600, 2011.

[13] Dipal Baruah and DC Baruah. Modeling of biomass gasification: a review. *Renewable and Sustainable Energy Reviews*, 39:806–815, 2014.

[14] Javier Gil, José Corella, Maria P Aznar, and Miguel A Caballero. Biomass gasification in atmospheric and bubbling fluidized bed: effect of the type of gasifying agent on the product distribution. *Biomass and Bioenergy*, 17(5):389–403, 1999.

[15] PN Rowe. Prediction of bubble size in a gas fluidised bed. *Chemical Engineering Science*, 31(4):285–288, 1976.

[16] Hina Beohar, Bhupendra Gupta, VK Sethi, and Mukesh Pandey. Parametric study of fixed bed biomass gasifier: a review. *International Journal of Thermal Technologies*, 2(1):134–140, 2012.

[17] Derek Geldart. Types of gas fluidization. *Powder technology*, 7(5):285–292, 1973.

[18] Fabrizio Scala. *Fluidized bed technologies for near-zero emission combustion and gasification*. Elsevier, 2013.

[19] Steffen Heidenreich and Pier Ugo Foscolo. New concepts in biomass gasification. *Progress in energy and combustion science*, 46:72–95, 2015.

[20] Erik Sette, David Pallarès, and Filip Johnsson. Experimental evaluation of lateral mixing of bulk solids in a fluid-dynamically down-scaled bubbling fluidized bed. *Powder Technology*, 263:74–80, 2014.

[21] L G_ Gibilaro and PN Rowe. A model for a segregating gas fluidised bed. *Chemical Engineering Science*, 29(6): 1403–1412, 1974.

[22] D Geldart. Single particles, fixed and quiescent beds. *Gas fluidization technology*, 2:11–32, 1986.

[23] Johanna Olsson, David Pallarès, and Filip Johnsson. Lateral fuel dispersion in a large-scale bubbling fluidized bed. *Chemical engineering science*, 74:148–159, 2012.

[24] Athirah Mohd Tamidi and Ku Zilati Ku Shaari. Effect of steam inlet velocity and solid initial bed height to the hydrodynamics of fluidized bed gasifier. *Journal of Applied Sciences(Faisalabad)*, 10(24):3257–3263, 2010.

[25] Peter McKendry. Energy production from biomass (part 1): overview of biomass. *Bioresource technology*, 83(1): 37–46, 2002.

[26] Meisam Farzaneh, Srdjan Sasic, Alf-Erik Almstedt, Filip Johnsson, and David Pallarès. A novel multigrid technique for lagrangian modeling of fuel mixing in fluidized beds. *Chemical engineering science*, 66(22):5628–5637, 2011.

[27] G Bruni, R Solimene, A Marzocchella, P Salatino, JG Yates, P Lettieri, and M Fiorentino. Self-segregation of high-volatile fuel particles during devolatilization in a fluidized bed reactor. *Powder Technology*, 128(1):11–21, 2002.

[28] R Bilbao, J Lezaun, M Menendez, and JC Abanades. Model of mixingsegregation for straw/sand mixtures in fluidized beds. *Powder technology*, 56(3):149–155, 1988.

[29] F Scala, R Chirone, and P Salatino. Attrition phenomena relevant to fluidized bed combustion and gasification systems. In *Fluidized Bed Technologies for Near-Zero Emission Combustion and Gasification*, pages 254–315. Elsevier, 2013.

[30] R Solimene, R Chirone, and P Salatino. Characterization of the devolatilization rate of solid fuels in fluidized beds by time-resolved pressure measurements. *AIChE Journal*, 58(2):632–645, 2012.

[31] Laihong Shen, Jun Xiao, Fredrik Niklasson, and Filip Johnsson. Biomass mixing in a fluidized bed biomass gasifier for hydrogen production. *Chemical Engineering Science*, 62(1-2):636–643, 2007.

[32] I Petersen and J Werther. Three-dimensional modeling of a circulating fluidized bed gasifier for sewage sludge. *Chemical Engineering Science*, 60(16):4469–4484, 2005.

[33] LG Gibilaro, K Gallucci, R Di Felice, and P Pagliai. On the apparent viscosity of a fluidized bed. *Chemical engineering science*, 62(1-2):294–300, 2007.

[34] JF Davidson. Harrison. d.: Fluidized particles, 1963.

[35] Shayan Karimipour and Todd Pugsley. A critical evaluation of literature correlations for predicting bubble size and velocity in gas–solid fluidized beds. *Powder Technology*, 205(1-3):1–14, 2011.

[36] Gui-Rong Liu and Moubin B Liu. *Smoothed particle hydrodynamics: a meshfree particle method*. World Scientific, 2003.